LIGO SURF Final Report:
Accurately Describing the Precession of Binary Black Holes with New Parameters

Charles F. A. Gibson [1,2] and Javier Roulet [1,3]

[1] LIGO, California Institute of Technology, Pasadena, CA 91125, USA

[2] Department of Physics, Allegheny College, Meadville, Pennsylvania 16335, USA

[3] TAPIR, Walter Burke Institute for Theoretical Physics, California Institute of Technology, Pasadena, CA 91125, USA

ABSTRACT

The precession of Binary Black Holes (BBHs) is dependent on the alignment of the orbital angular momentum and total spin; precession becomes stronger with higher misalignment of the total spin and orbital angular momentum. Weakly precessing systems are likely to have formed through binary stellar evolution, while strongly precessing systems may have been formed dynamically. Despite the growing number of LIGO sources, evidence of precession is strongly debated in the literature. The parameter χ_{p} is currently used to evaluate the precession of observed BBH systems. However, χ_{p} is difficult to constrain to a narrow range of values for most events, and furthermore under commonly used priors its probability density vanishes at the aligned-spin configuration $\chi_{\mathrm{p}} = 0$. We present an alternative spin precession parameter, the cosine of the angle between the total spin and the orbital angular momentum $\cos\theta_{\mathrm{LS}}$, that provides better localization of a precession value and allows a non-zero probability of aligned spins. We begin by testing $\cos\theta_{\mathrm{LS}}$, χ_{p}, and other parameters against synthetic data with known values to determine the best statistical measurement of precession. We then use $\cos\theta_{\mathrm{LS}}$ to evaluate the precession in events from O3.

1. MOTIVATION

The properties of binary black hole (BBH) mergers observed from LIGO-Virgo-KAGRA detections can be informative of the formation channel of the system (e.g., Mandel & Farmer 2022). Two primary theories of the origin of BBHs exist. The first is that the systems were formed through stellar evolutionary channels. Namely, as a binary system between two intermediately massive stars evolved, both stars remained in orbit, with the resulting black holes (BHs) surviving the supernovae at the end of the stars' lives. Eventually, due to the emission of gravitational waves (GWs), the two coalesced into a single BH through a BH-BH merger.

Alternatively, the BBH system may have been formed dynamically. Through the gravitational interactions of stars and black holes in dense stellar environments such as globular clusters and galactic nuclei, scattering events can place two, previously unrelated BHs into orbit around each other. This would most likely be from a three-body interaction in which an intruding BH kicks a less massive companion from a the binary the other BH is in, yielding a BBH system.

One way to potentially differentiate between these two formation channels is through analyzing the precession of the orbit. The BHs in BBH systems that formed from binary stellar evolution likely have spins $\vec{S}$ that are approximately aligned with the orbital angular momentum $\vec{L}$. This stems from the preferential alignment of stellar rotation axes with the $\vec{L}$ of the binary, initialized by the angular momentum in stellar nurseries. Additional complications such as kicks from the supernovae of companion stars in the binary may misalign spins. However, the details of these processes are still not well modeled, so approximations to the effects must be taken into account. The simplest of approximations neglect these kicks, claiming that $\vec{S}$ and $\vec{L}$ remain aligned through the entire binary evolution process through the BBH merger.

Conversely, dynamically formed BBH systems are much more likely to have isotropic spin distributions. Because there is no initial relationship between $\vec{S}$ and $\vec{L}$, any orientation of the alignment of $\vec{S}$ and $\vec{L}$ is equally likely. This assumption leads to the prediction that the orbits of dynamically formed BBH systems are more likely to precess than the orbits of binary stellar evolution remnants.

By understanding the precession of a BBH system, information regarding the formation channel of the binary can be gleaned. In particular, analyzing the precession found in LIGO-Virgo data from O1, O2, and O3 can help inform predictions of the origins of known BBH

merger candidates. With just under 100 candidates of BBH systems as of O3 (Abbott et al. 2023; Mehta et al. 2023; Nitz et al. 2023), statistical conclusions can begin to be made about the nature of BBH precession and, therefore, the origin of the BBH systems. These conclusions may be especially useful in understanding the nature of binary evolution, dense stellar environments, and dynamical interactions.

Currently, there exists a parameter χ_{p} that has been used to describe the precession of the orbit. However, claims of individual precessing candidates are controversial (Hannam et al. 2022; Payne et al. 2022). The evidence for precession in these individual events is inconclusive because χ_{p} is not very informative. The issues with χ_{p} are described in detail in Section 2. This summer, we focus on defining a new parameter that can better constrain orbital precession of BBH systems. We begin by detailing the cause of controversy from χ_{p} in Section 2 before defining new parameters in Section 3. We then outline the statistical tests used to constrain the parameter in Section 4. We choose our parameter in Section 5 and apply it to LIGO data in Section 6.

2. PROBLEM

The effective precession parameter currently used to describe the precession of a BBH system, χ_{p}, is defined as

$$\chi_{\mathrm{p}} = \max\left(\chi_1 \sin\theta_{S_1L}, \frac{q(4q+3)}{3q+4}\chi_2 \sin\theta_{S_2L}\right), \quad (1)$$

where χ_i is the dimensionless spin parameter of the BH i, q is the mass ratio m_2/m_1 (where $m_1 > m_2$), and θ_{S_iL} is the angle between the spin $\vec{S}$ of BH i and the orbital angular momentum $\vec{L}$ (Schmidt et al. 2015). This quantity is geometrically defined as the maximum in-plane spin contribution (Schmidt et al. 2015). When $\chi_{\mathrm{p}} = 0$, the system is not precessing, and when $\chi_{\mathrm{p}} = 1$, the system is strongly precessing.

When using this parameter with the express purpose of determining precession of individual events, there are two main issues: The first can be seen by the posterior distributions in Figure 1. Most of the posterior distributions for χ_{p} are very broad. A broad posterior distribution is not very informative on the true value associated with the data, as it makes it difficult to constrain it. The second is displayed by the prior distribution in Figure 1: the prior distribution $\pi(\chi_{\mathrm{p}})$ sharply approaches 0 as χ_{p} approaches 0.

The first issue makes χ_{p} a poor parameter statistically. The second issue makes it hard to interpret whether aligned spins are consistent with the data from the χ_{p} posterior. However, by initially assuming the spins are
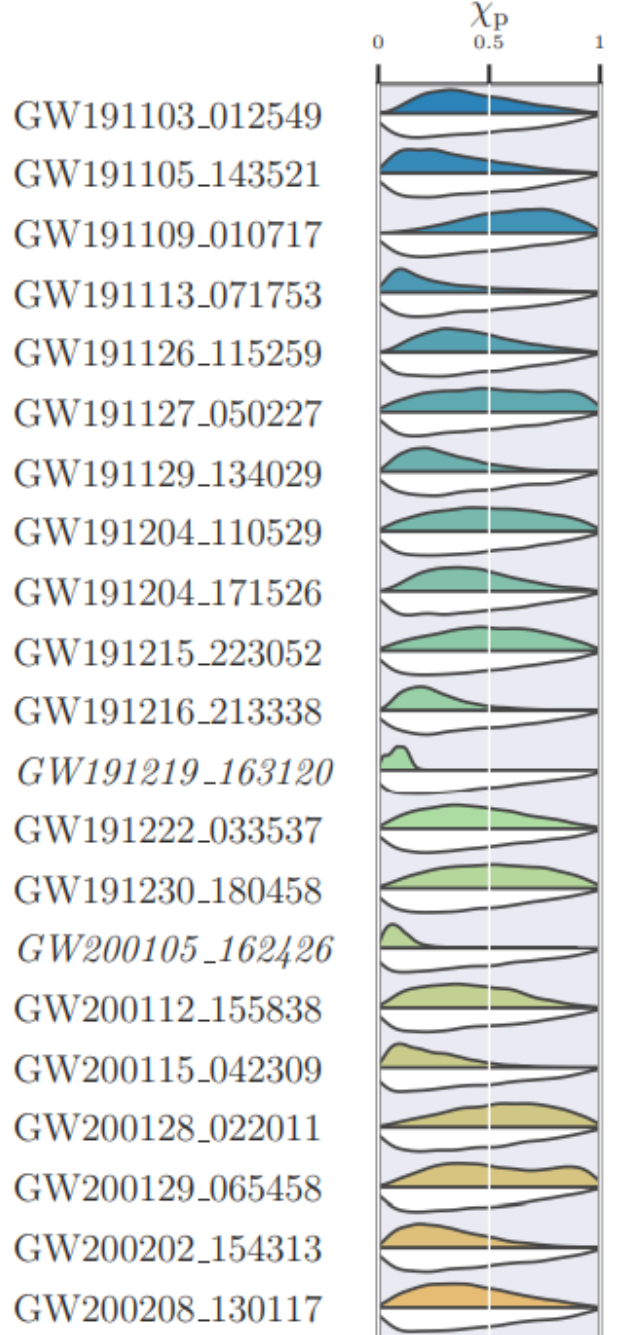
Figure 1. The χ_{p} distributions of several observations from Abbott et al. (2023). Note that most of the posteriors (upper curves) are very broad, only marginally differing from the prior distribution (lower curves). For the more localized posteriors, the localization only occurs at low values of χ_{p} where the peak in the prior occurs, and these events have high levels of uncertainty of astrophysical origin.

misaligned (as the probability of alignment is 0 in the prior in χ_{p}), the parameter fails to reject aligned spins. This is because the posterior distribution is defined as the prior distribution times the likelihood, so if the prior
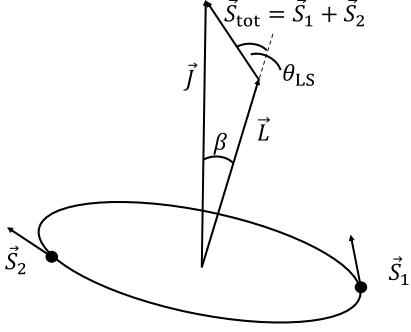
Figure 2. The geometry of a BBH system. The spins of each black hole are denoted by $\vec{S}_i$ (with the total spin $S_{\text{tot}} = \vec{S}_1 + \vec{S}_2$), the orbital angular momentum is expressed as $\vec{L}$, and the total angular momentum $(\vec{L} + \vec{S}_1 + \vec{S}_2)$ is $\vec{J}$. θ_{LS} is the angle between $\vec{L}$ and $\vec{S}_{\text{tot}}$. β is the angle between $\vec{J}$ and $\vec{L}$.

is 0 at a value, then the posterior will always be 0 at that value.

In this work, we aim to propose an alternative parameter that addresses these two issues. Namely, we want a parameter that has a narrow posterior distribution, and whose prior density does not vanish for aligned spins.

3. SELECTED PARAMETERS FOR TESTING

Using the geometry of the BBH merger outlined in Figure 2, two alternative parameters were initially selected. First is θ_{LS}, the angle between $\vec{L}$ and the total spin $\vec{S}_{\text{tot}} = \vec{S}_1 + \vec{S}_2$. This angle provides a direct geometric understanding of the relationship between $\vec{S}_{\text{tot}}$ and $\vec{L}$, fundamentally relating to the orbital precession. The second is β, the angle between $\vec{L}$ and the total angular momentum $\vec{J} = \vec{S}_{\text{tot}} + \vec{L}$. β is especially promising because, as a precession indicator, it impacts the magnitude modulations and phase evolution of the waveform (Fairhurst et al. 2020). Particularly, the parameter $b = \tan(\beta/2)$ is directly used to compute the waveform. However, unlike β, θ_{LS}, and χ_{p}, b has infinite bounds, making it more difficult to constrain a "maximum" precession for the system. Regardless, θ_{LS} and β share the same statistical issue with χ_{p}: their probability densities of both parameters tend towards zero when $\vec{S}$ and $\vec{L}$ are aligned. To address this issue, we instead consider the cosine of the angles, $\cos\theta_{\text{LS}}$ and $\cos\beta$. This coordinate shift to cosine is chosen because it yields a non-zero probability density of aligned spins in the prior.

4. TESTING EACH PARAMETER
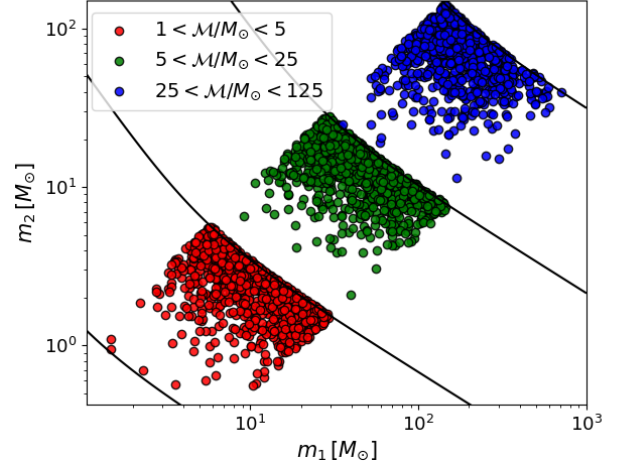
Figure 3. The distribution of the chirp mass for the ~ 3000 injections used to construct the posteriors.

4.1. Constructing the Initial Parameter Test

In order to measure how informative the three parameters (χ_{p}, $\cos\theta_{\text{LS}}$, and $\cos\beta$) are, we needed to test them on known values. As the exact values of the main parameters from LIGO-Virgo-KAGRA sources are not known, we instead used synthetic data with posteriors formed from known injections. These injections were generated assuming an isotropic spin distribution. That is, all true angles between $\vec{L}$ and $\vec{S}$ are equally likely in the synthetic data. We used sampled posterior distributions for roughly 3000 known injections from a previous work to begin our analysis.[1] These injections were sorted into three mass distributions based on the chirp mass $\mathcal{M}$ of the BBH. The three $\mathcal{M}$ distributions are shown in Figure 3, where we consider low mass to be $1 < \mathcal{M}/M_\odot < 5$, mid mass to be $5 \leq \mathcal{M}/M_\odot < 25$, and high mass to be $25 \leq \mathcal{M}/M_\odot < 125$.

Each point on Figure 3 corresponds to a different injected event. Using the sampled posterior distribution of base parameters of the events, we constructed posteriors of our new precession parameters: χ_{p}, $\cos\theta_{\text{LS}}$, and $\cos\beta$.

4.2. Methods of Statistical Analysis of Injections

Due to the large number of samples, it became necessary to find a way to summarize all the information present in the posterior distributions of each event.

Our new parameter aims to address two hypotheses: $\vec{S}_{\text{tot}}$ is either aligned with $\vec{L}$, or randomly oriented with

respect to it. Across many events, this corresponds to an aligned or isotropic spin distribution. We use the Neyman-Pearson Lemma to compare these two hypotheses.

This is the strongest statistical test for distinguishing between two hypotheses $\mathcal{H}_0$ and $\mathcal{H}_1$. The test is defined as the likelihood ratio of the hypotheses, expressed as

$$\Lambda = \frac{p(d \mid \mathcal{H}_1)}{p(d \mid \mathcal{H}_0)} \qquad (2)$$

(Neyman & Pearson 1933).

If the likelihoods are the same, then the ratio is equal to 1 and there is no difference between the hypotheses. Alternatively, if the likelihood of $\mathcal{H}_1$ is greater than the likelihood of $\mathcal{H}_0$, then $\mathcal{H}_1$ is more likely to be true. Some minimum threshold of Λ might be set to confirm if a given hypothesis is confidently true.

We can express each hypothesis as a specific set of individual parameters:

$$\mathcal{H}_0 : \theta \sim \pi(\theta) \qquad (3)$$
$$\mathcal{H}_1 : \theta = \theta_*. \qquad (4)$$

$\mathcal{H}_0$ is expressed as a distribution of θ values, corresponding to an isotropic spin distribution. $\mathcal{H}_1$ is a specific case of the isotropic spin distribution that yields aligned $\vec{S}$ and $\vec{L}$.

Using the relationship between the likelihood $\mathcal{L}$, the posterior $\mathcal{P}$, the prior π, and the evidence $\mathcal{Z}$,

$$\mathcal{P} = \frac{\mathcal{L}\pi}{\mathcal{Z}} \qquad (5)$$

and the definitions of $\mathcal{H}_0$ and $\mathcal{H}_1$, we can express the likelihood $p(d \mid \mathcal{H}_1)$ as

$$p(d \mid \mathcal{H}_1) = p(d \mid \theta_*) \qquad (6)$$
$$p(d \mid \theta_*) = \mathcal{L} \qquad (7)$$
$$\mathcal{L} = \frac{p(\theta_* \mid d, \mathcal{H}_0)\, p(d \mid \mathcal{H}_0)}{\pi(\theta_* \mid \mathcal{H}_0)}. \qquad (8)$$

Plugging this into Equation (2), we get

$$\frac{p(\theta_* \mid d, \mathcal{H}_0)}{\pi(\theta_* \mid \mathcal{H}_0)}. \qquad (9)$$

However, a BBH system is not 1-dimensional, as it is defined by many parameters. Although precession is not necessarily based on a single parameter, our goal is to find a single parameter that can provide significant information on the precession of the system. We can express θ as a multidimensional parameter that contains a single parameter x that exclusively preserves the relevant precession information and all other unrelated parameters θ' as

$$\theta = (x, \theta') \qquad (10)$$

We can then define a new hypothesis $\tilde{\mathcal{H}}_1$ that remains as close to $\mathcal{H}_1$ as possible while only being based on a single parameter. This effectively makes the simplifying assumption that all the relevant precession information is contained within a single parameter. Under this assumption, $\tilde{\mathcal{H}}_1$ should be identical to $\mathcal{H}_0$ with the exception of the precession parameter x. Ideally, there should only be one value of x, x_*, where $\mathcal{H}_0$ reduces to $\tilde{\mathcal{H}}_1$. That is, in an isotropic spin distribution, only one orientation of the vectors yields aligned $\vec{S}_{\mathrm{tot}}$ with $\vec{L}$.[2] We can express this assumption as

$$\pi(\theta' \mid x_*, \tilde{\mathcal{H}}_1) = \pi(\theta' \mid x_*, \mathcal{H}_0) \qquad (11)$$

and thus,

$$\pi(\theta \mid x_*, \tilde{\mathcal{H}}_1) = \delta(x - x_*)\pi(\theta' \mid x_*, \mathcal{H}_0). \qquad (12)$$

It then follows that $p(d \mid \mathcal{H}_1) \approx p(d \mid \tilde{\mathcal{H}}_1)$. Using the same process as in Equations (6–8), we can express $p(d \mid \tilde{\mathcal{H}}_1)$ as

$$p(d \mid \tilde{\mathcal{H}}_1) = p(d \mid x_*, \tilde{\mathcal{H}}_1) \qquad (13)$$
$$= p(d \mid x_*, \mathcal{H}_0) \qquad (14)$$
$$= \frac{p(x_* \mid d, \mathcal{H}_0)p(d \mid \mathcal{H}_0)}{\pi(x_* \mid \mathcal{H}_0)}, \qquad (15)$$

and plugging Equation (15) into Equation (2), we get the revised ratio

$$\Lambda = \frac{p(d \mid \tilde{\mathcal{H}}_1)}{p(d \mid \mathcal{H}_0)} \qquad (16)$$
$$= \frac{\frac{p(x_* \mid d,\ \mathcal{H}_0)p(d \mid \mathcal{H}_0)}{\pi(x_* \mid \mathcal{H}_0)}}{p(d \mid \mathcal{H}_0)} \qquad (17)$$
$$= \frac{p(x_* \mid d, \mathcal{H}_0)}{\pi(x_* \mid \mathcal{H}_0)} \qquad (18)$$

This ratio, called the Savage-Dickey Ratio (SDR), provides a simpler way to compare the competing hypotheses that are expressed through a single parameter, allowing for a more quantitative way to evaluate the most informative parameter on the alignment of $\vec{S}_{\mathrm{tot}}$ and $\vec{L}$. The most informative parameter should have high SDR values for events where $\vec{S}_{\mathrm{tot}}$ and $\vec{L}$ are truly aligned and it should have low SDR values for events where $\vec{S}_{\mathrm{tot}}$ and $\vec{L}$ are truly misaligned.

---

[2] This approximation does neglect some information. For example, if the two spins having vertical components of $\vec{S}$ that align with $\vec{L}$ but the horizontal components of their spins cancel, this assumption fails to identify the spin misalignment in the system.
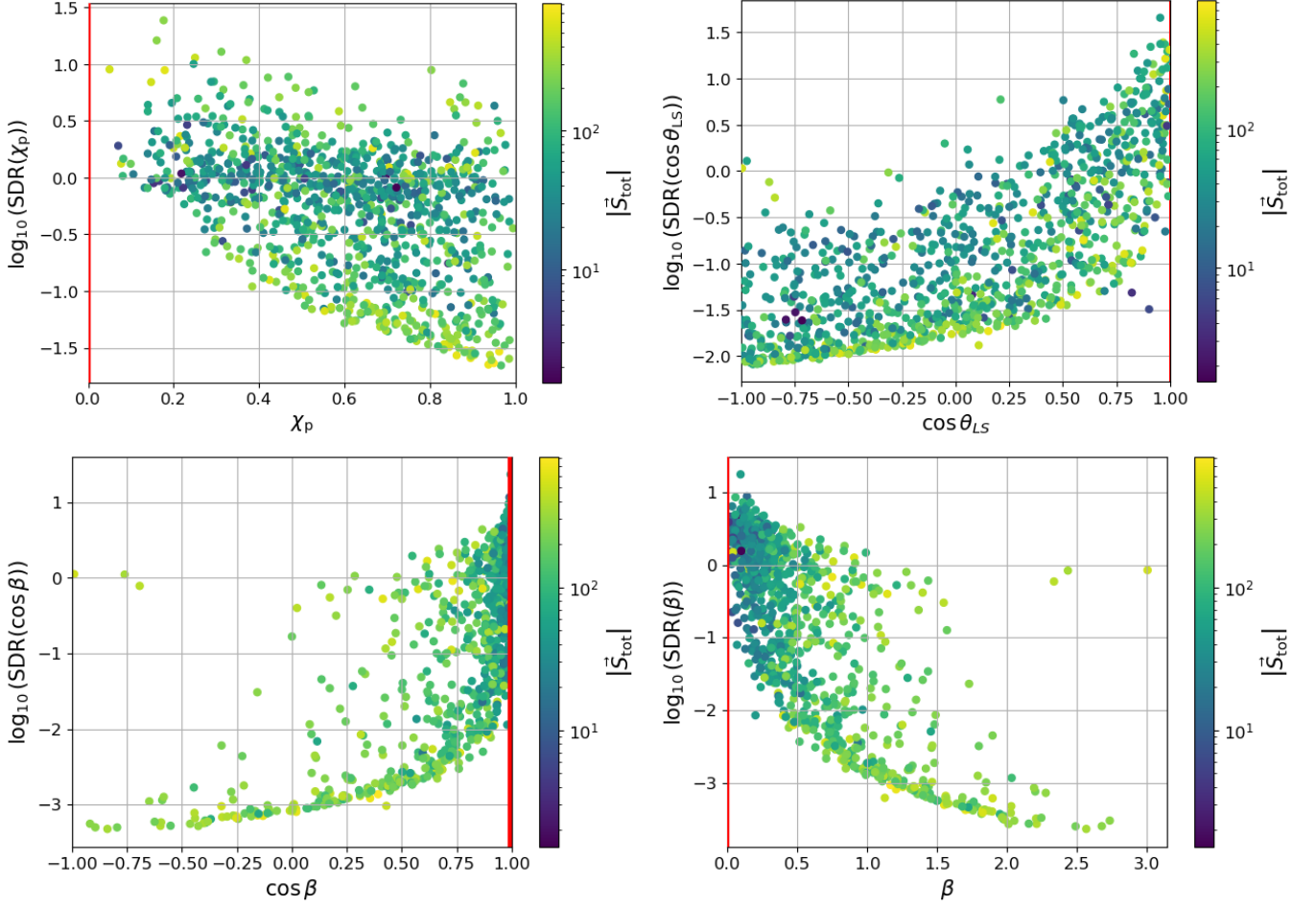
Figure 4. Savage-Dickey ratios for four tested parameters. Each point represents an injection and associated parameter estimation. The SDR used is between the hypotheses that the spins are aligned rather than isotropic. The true, injected value is on the horizontal axis, while the Savage–Dickey ratio is on the vertical axis. The color bar symbolizes the strength of the strength of the total spin $\vec{S}_{\text{tot}}$. The likelihood ratio for χ_{p} is strongly clustered around values ranging from ~ 1, making it a poor test of spin alignment. Meanwhile, the likelihood ratio for $\cos\theta_{\text{LS}}$ is slightly more informative. Because it spans several orders of magnitude, strongly precessing BBH systems ($\cos\theta_{\text{LS}} \sim -1$) would be much more likely than weakly precessing systems to be ruled out as having aligned spins. β and $\cos\beta$ have maximum SDR values similar to those of $\cos\theta_{\text{LS}}$ but much lower SDRs for highly misaligned cases.

²⁵⁸ We summarize the SDR data for each parameter in
²⁵⁹ Figure 4. We demonstrate in a more quantitative way
²⁶⁰ that the distribution of χ_{p} for most events are not
²⁶¹ very informative. However, it is more difficult to deter-
²⁶² mine if $\cos\beta$ or $\cos\theta_{\text{LS}}$ is a better parameter at distin-
²⁶³ guishing aligned vs misaligned $\vec{S}_{\text{tot}}$ and $\vec{L}$. Regardless,
²⁶⁴ this initial analysis provides a strong incentive to eval-
²⁶⁵ uate the orbital precession of individual LIGO-Virgo-
²⁶⁶ KAGRA sources using $\cos\theta_{\text{LS}}$ or $\cos\beta$ in place of χ_{p}.

4.3. *Numerical Difficulties in Calculating the Savage-Dickey Ratio*

²⁶⁹ The second issue with χ_{p} outlined in Section 2 stated
²⁷⁰ that the prior approached 0 for the case of aligned $\vec{S}_{\text{tot}}$
²⁷¹ and $\vec{L}$. This also makes the posterior distribution ap-
²⁷² proach 0 for aligned $\vec{S}_{\text{tot}}$ and $\vec{L}$. This means that we
²⁷³ obtain an indeterminate form of $\frac{0}{0}$ when taking the limit

$$\lim_{\beta,b,\chi_{\text{P}}\to 0} \frac{p(\text{AlignedSpins} \mid d)}{\pi(\text{AlignedSpins})} \to \frac{0}{0}. \tag{19}$$

²⁷⁵ When using L'Hôpital's Rule and differentiating the
²⁷⁶ numerator and denominator of the posterior and prior
²⁷⁷ in the limit, we can avoid numerical difficulties in cal-
²⁷⁸ culating the SDR, as we can avoid having the ratio of
²⁷⁹ $\frac{0}{0}$ when calculating the SDRs. Ultimately, we can re-
²⁸⁰ express the limit as

$$\lim_{\beta,b,\chi_{\text{P}}\to 0} \frac{p'(\text{AlignedSpins} \mid d)}{\pi'(\text{AlignedSpins})}. \tag{20}$$

²⁸² Under the assumption that the distributions of χ_{p}, β,
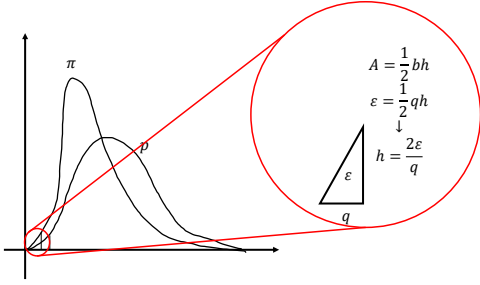
Figure 5. The geometry used to derive Equation (21).

and b are triangular very close to 0, we can geometrically express the value of p' and π'. Figure 5 demonstrates the geometry of the two curves. By finding the value of the parameter q_p (q_π) whose posterior (prior) distribution contains the area ε, we can express the ratio in the limit as

$$\frac{p'}{\pi'} = \frac{q_\pi^2}{q_p^2}. \tag{21}$$

When employing this alternative expression of the SDR, we can avoid numerical difficulties that arise from the properties of the prior distribution. We also find that the SDRs from this ratio are relatively insensitive to the ε that when ε is small ($\varepsilon = 0.003,\ 0.005,\ 0.007,\ 0.01$).

4.4. *Selection Effects in the Synthetic Posteriors*

As mentioned earlier, the synthetic data was generated based on an isotropic distribution of spin angles. However, the injections were also filtered to only allow events that would have signals recognizable by LIGO. As the mass of the BHs in the system increase, selection effects begin to occur. Most notably, the frequency of the BBH merger f_{merger} is inversely proportional to the mass, where $f_{\mathrm{merger}} \propto 1/M$. This means that more massive BBHs merge at lower frequencies. The alignment of $\vec{S}$ and $\vec{L}$ also affects the frequency of the merger: highly misaligned $\vec{S}$ and $\vec{L}$ merge more quickly at lower frequencies. These two effects cause the final frequency of high-mass, strongly precessing mergers to occur at low frequencies, potentially being undetectable by LIGO. Figure 6 outlines the distribution of the injected $\cos\theta_{\mathrm{LS}}$ used to approximate the priors used for the SDRs of each parameter.

5. CHOOSING A PARAMETER

5.1. *Evaluating the Divergence of Isotropic and Aligned Spin Distributions*

Although χ_{P} seems to be less informative than $\cos\beta$ and $\cos\theta_{\mathrm{LS}}$ by looking at the trend of the SDRs, it became difficult to compare the effectiveness of $\cos\beta$ or
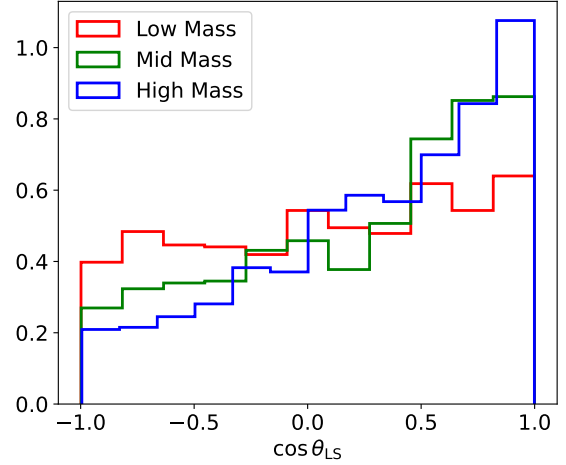
Figure 6. The probability density distribution of injections for the three mass distributions. The data was initially generated to have a flat prior regardless of mass, but as the mass increases, the probability density of having aligned $\vec{S}$ and $\vec{L}$ increase. This is due to the filtering of events that exclusively selects events that can be detected by LIGO, as described in Section 4.4.

$\cos\theta_{\mathrm{LS}}$ as they are both relatively effective. We have just over 1000 synthetic posteriors for each of the three mass distributions, leaving over 3000 SDR values. One way to summarize the effectiveness of each parameter across all samples is to measure the Kullback-Leibler divergence D_{KL}, a test that evaluates the difference between two distributions. In particular, we used this to evaluate the difference between the likelihoods of aligned and isotropic spin distributions. By maximizing D_{KL} between the two distributions with our parameter, we could find the parameter that yields the most divergent set of distributions. The Kullback-Leibler divergence between these two likelihoods is defined as

$$D_{\mathrm{KL}}(p(d \mid \mathcal{H}_0) \parallel p(d \mid \tilde{\mathcal{H}}_1))$$
$$= \int \mathrm{d}d\, p(d \mid \mathcal{H}_0) \log_2 \frac{p(d \mid \mathcal{H}_0)}{p(d \mid \tilde{\mathcal{H}}_1)}, \tag{22}$$

which can be approximated as

$$D_{\mathrm{KL}} \approx \frac{1}{N} \sum_{d_j \sim \mathcal{H}_0} \log_2 \frac{p(d_j \mid \mathcal{H}_0)}{p(d \mid \tilde{\mathcal{H}}_1)}. \tag{23}$$

However, we have shown in Equations (16–18) that the inverse of this ratio of likelihoods can be approximated as the Savage-Dickey Ratio, the ratio of the posterior to the prior. Incorporating this result, we can express the

Table 1. $D_{\mathrm{KL}}(p(d \mid \mathcal{H}_0) \parallel p(d \mid \tilde{\mathcal{H}}_1))$

Mass	χ_{p}	$\cos\theta_{\mathrm{LS}}$	β	$\cos\beta$	b
Low	1.01 ± 0.06	2.97 ± 0.09	2.86 ± 0.13	2.42 ± 0.13	2.93 ± 0.13
Mid	1.69 ± 0.06	2.92 ± 0.09	1.76 ± 0.11	2.05 ± 0.11	1.79 ± 0.11
High	0.94 ± 0.04	1.99 ± 0.08	0.92 ± 0.08	0.99 ± 0.08	0.93 ± 0.08

Notes: The D_{KL} values of each parameter (measured in bits) comparing the distributions of aligned to isotropic spins. The "Mass" column corresponds to one of three mass distributions of the injections used to construct the posteriors.

divergence as

$$D_{\mathrm{KL}} \approx \frac{1}{N} \sum_{d_j \sim \mathcal{H}_0} \log_2 \frac{\pi(x_* \mid \mathcal{H}_0)}{p(x_* \mid d, \mathcal{H}_0)} \qquad (24)$$

$$= -\frac{1}{N} \sum_{d_j \sim \mathcal{H}_0} \log_2 \mathrm{SDR}. \qquad (25)$$

The D_{KL} values for each parameter across the three distributions used in this study are reported in Table 1. χ_{p} consistently has the lowest D_{KL} while $\cos\theta_{\mathrm{LS}}$ consistently has the highest. This means that χ_{p} is the least effective at distinguishing between the isotropic and aligned spin distributions while $\cos\theta_{\mathrm{LS}}$ is the best. We expect $D_{\mathrm{KL}}(\beta) = D_{\mathrm{KL}}(\cos\beta) = D_{\mathrm{KL}}(b)$ as they are just different coordinate expressions of β, but this is not the case. This suggests that our numerical computation has limited accuracy. Regardless, none of the D_{KL} values for any coordinate of β in any mass distribution are greater than that of $\cos\theta_{\mathrm{LS}}$. Additionally, as the distribution goes to higher masses, it becomes more difficult to distinguish between isotropic and aligned spins, especially between β and χ_{p}.

Given these results, it appears that $\cos\theta_{\mathrm{LS}}$ is the strongest parameter at distinguishing misaligned spins from aligned spins, while χ_{p} is the weakest.

5.2. *Relationship to Other Parameters*

Although $\cos\theta_{\mathrm{LS}}$ appears to most accurately diagnose the precession of a BBH system, it is important to compare it to other parameters. We have already shown that the mass of the BBH system influences which events may be detected by LIGO. However, its relationship with the total spin should also be considered. Figure 4 demonstrates that $\cos\theta_{\mathrm{LS}}$ is more effective at rejecting aligned spins for misaligned systems with a high total spin.

6. UTILIZING LIGO DATA

By identifying triggers with high p_{astro} through a population model, we then evaluated events that are aligned with those in the IAS catalog (Olsen et al. 2022). Assuming a flat prior for $\cos\theta_{\mathrm{LS}}$ (this time with no selection effects as with the earlier injected data), we sampled each event to construct a posterior distribution of each parameter.

The D_{KL} of $\cos\theta_{\mathrm{LS}}$ provides evidence that $\cos\theta_{\mathrm{LS}}$ is the most informative of the tested parameters. By constructing posterior distributions of $\cos\theta_{\mathrm{LS}}$, we can evaluate if any individual events are precessing. Narrow posterior distributions that reject alignment are ideal for providing strong evidence of precession in an individual candidate. Conversely, narrow posterior distributions that include alignment would provide evidence for no precession, and broad distributions make it difficult to interpret the state of the system's precession. We provide the posterior distributions of $\cos\theta_{\mathrm{LS}}$ and χ_{p} for each event in O3a in Figure 7.

Recall that an SDR with high values corresponds to events that are likely not precessing, low SDRs correspond to events with high precession. We calculate the SDR using the reconstructed posterior distributions and flat $\cos\theta_{\mathrm{LS}}$ prior. Figure 8 demonstrates two things about the O3a data: there is a broader range of SDRs for $\cos\theta_{\mathrm{LS}}$, meaning that $\cos\theta_{\mathrm{LS}}$ can more strongly support or reject precession (as shown with the D_{KL} values), and there are individual events that have stronger evidence for precession as obtained by the posterior when using $\cos\theta_{\mathrm{LS}}$ instead of χ_{p}.

Ultimately, the events with the lowest SDR values may be the most likely to be precessing. These events, with high levels of confidence, are GW190408_181802, GW190915_235702, GW190707_093326, and GW190421_213856.

Each event with evidence of precession has marginal significance, meaning that we cannot make claims of individual precession on the events that we have currently analyzed.

7. CONCLUSION

Overall, we provided a series of statistical tests to determine a stronger parameter for determining the precession of individual events. Using these methods, we found that $\cos\theta_{\mathrm{LS}}$ was more informative than χ_{p} for these purposes. Using $\cos\theta_{\mathrm{LS}}$, we could identify events that may be precessing with higher confidence than with χ_{p}. We would like to analyze events from additional runs such as O3b and O2. We would also like to employ future work to study the overall population of spin-orbital angular momentum alignment will be completed. This can be informative on the true distribution of spin-orbital angular momentum, ultimately providing hints into the formation channel of binary black hole systems.
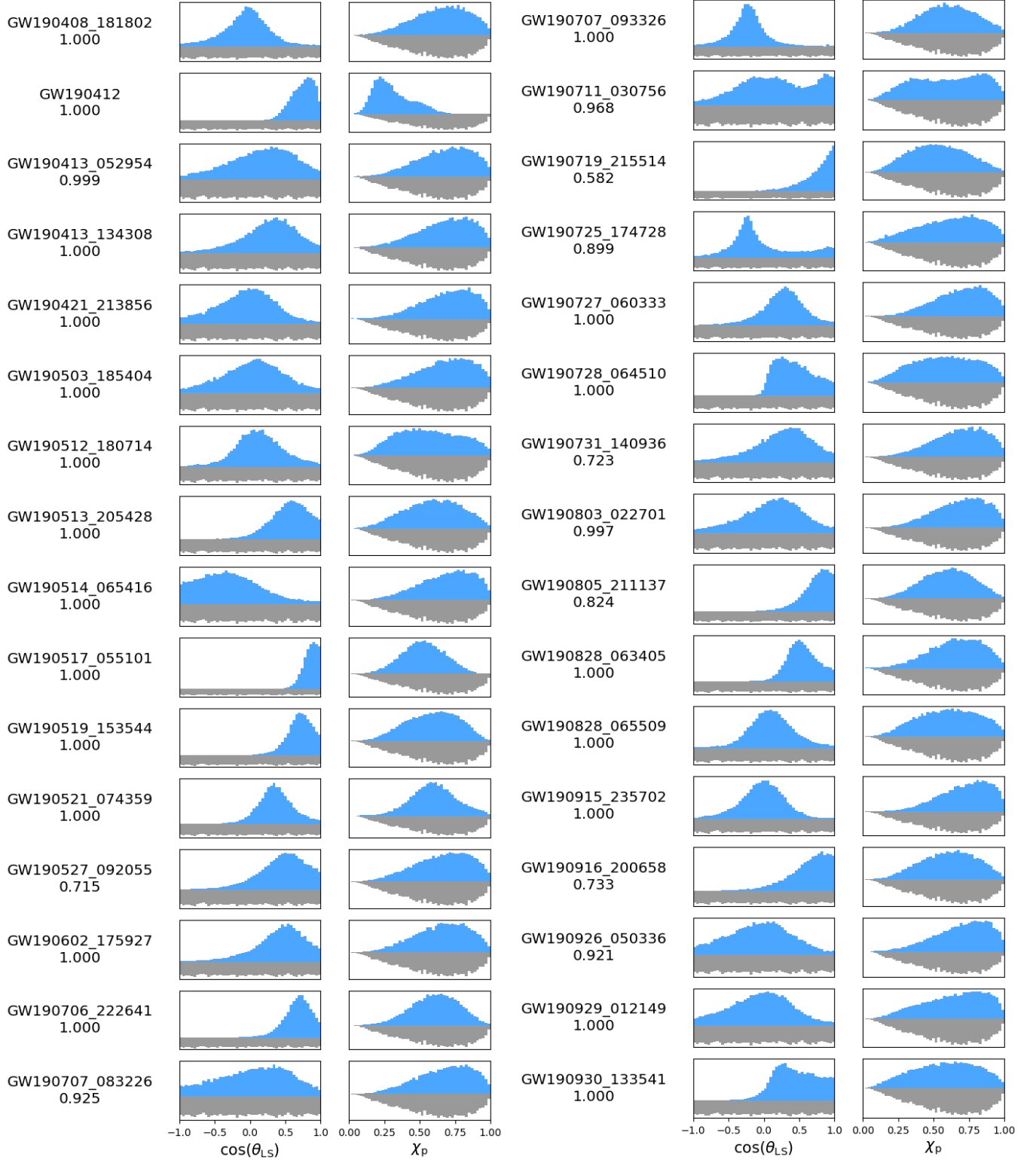
Figure 7. The posterior distributions (blue) of $\cos\theta_{\mathrm{LS}}$ and χ_{p} against the prior distributions (gray) of the events in O3a as we found in our population model. We use a modified IAS Pipeline to include events with $p_{\mathrm{astro}} > 0.5$. The distributions of χ_{p} are broad and resemble the priors, while the posteriors of $\cos\theta_{\mathrm{LS}}$ tend to be more localized in some cases. The probability of astrophysical origin, p_{astro} is included below the event name.
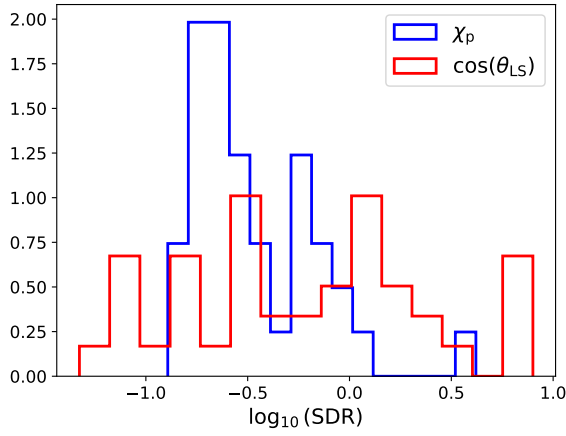
Figure 8. A histogram of the Savage-Dickey Ratios of $\chi_{\rm p}$ and $\cos\theta_{\rm LS}$, calculated from the posterior distributions from the events in the catalogue from our population inference.

REFERENCES

Abbott, R., Abbott, T. D., Acernese, F., et al. 2023, Physical Review X, 13, 041039, doi: 10.1103/PhysRevX.13.041039

Fairhurst, S., Green, R., Hoy, C., Hannam, M., & Muir, A. 2020, PhRvD, 102, 024055, doi: 10.1103/PhysRevD.102.024055

Hannam, M., Hoy, C., Thompson, J. E., et al. 2022, Nature, 610, 652, doi: 10.1038/s41586-022-05212-z

Mandel, I., & Farmer, A. 2022, PhR, 955, 1, doi: 10.1016/j.physrep.2022.01.003

Mehta, A. K., Olsen, S., Wadekar, D., et al. 2023, arXiv e-prints, arXiv:2311.06061, doi: 10.48550/arXiv.2311.06061

Neyman, J., & Pearson, E. S. 1933, Philosophical Transactions of the Royal Society of London Series A, 231, 289, doi: 10.1098/rsta.1933.0009

Nitz, A. H., Kumar, S., Wang, Y.-F., et al. 2023, ApJ, 946, 59, doi: 10.3847/1538-4357/aca591

Olsen, S., Venumadhav, T., Mushkin, J., et al. 2022, PhRvD, 106, 043009, doi: 10.1103/PhysRevD.106.043009

Payne, E., Hourihane, S., Golomb, J., et al. 2022, PhRvD, 106, 104017, doi: 10.1103/PhysRevD.106.104017

Schmidt, P., Ohme, F., & Hannam, M. 2015, PhRvD, 91, 024043, doi: 10.1103/PhysRevD.91.024043